Electronic and optical properties of body-centered-tetragonal Si and Ge

Brad D. Malone,* Steven G. Louie, and Marvin L. Cohen
Department of Physics, University of California, Berkeley, California 94720, USA and Material Sciences Division, Lawrence Berkeley National Laboratory, Berkeley, California 94720, USA

(Received 24 July 2009; revised manuscript received 10 December 2009; published 1 March 2010)

We present a first-principles calculation of the quasiparticle and optical excitation spectra of recently predicted silicon and germanium polytypes in the body-centered-tetragonal (bct) structure. The quasiparticle spectra calculated within the *GW* approximation predict that both silicon and germanium in the bct structure are small band gap materials with indirect gaps of 0.86 and 0.38 eV, respectively. The optical spectra is evaluated by solving the Bethe-Salpeter equation taking into account electron-hole interactions. We then make comparison to the cubic phases of Si and Ge which suggest the possible utility of the silicon bct phase in photovoltaic applications.

DOI: 10.1103/PhysRevB.81.115201 PACS number(s): 78.20.Bh, 71.20.Mq

I. INTRODUCTION

Silicon and germanium play an important role in countless electronic and photovoltaic devices that are at the heart of modern technological development. Their importance necessitates an understanding of their properties, in particular their electronic and optical characteristics. The cubic phases of both of these materials have been extensively studied over the years and have been the topic of a large number of publications. However, while much about the cubic phases is known, much less is known about the various polytypes that these elements form. The interest in obtaining a better understanding of the other polytypes that these materials form is not only interesting from a scientific perspective, but because a number of these phases have common characteristics with their cubic counterparts they may have possible applications in the same domains of use. Additionally, many of these phases are the subject of current experimental study and thus a good theoretical understanding of these materials is desired.

One of the most recent developments in the understanding of the phase diagram of silicon and germanium has been the prediction of a new fourfold coordinated phase in the body-centered tetragonal (bct) structure.[1] This phase had been recently discovered in studies of carbon through molecular-dynamics simulations as a crystalline phase that carbon nanotubes form under a pressure of 20 GPa.[2] Because of the similarities between the group-IVA materials, this phase was expected to occur for silicon and germanium. The *ab initio* calculations performed in the first study of the bct Si and Ge structures suggest that this structure would be metastable with a total energy higher than the cubic structure by only $\sim$0.1 eV/atom.[1] Upon the inclusion of quasiparticle corrections using the *GW* approximation (GWA) (Refs. 3 and 4) silicon in the bct structure was found to be semiconducting with an indirect band gap of 0.47 eV.[1] Germanium, on the other hand, was found to have an indirect overlap in the local-density approximation (LDA) which persists even after the quasiparticle corrections. While the bct phase in Si and Ge has yet to be observed experimentally, it has been suggested that a possible path for obtaining this structure is heteroepitaxial growth on the (111) surface of a Ge substrate in the case of Si and the (111) surface of a Ge-Sn buffer layer in the case of Ge.[1]

The discovery of a small band gap silicon polytype motivates an interest in its optical properties since silicon-based materials currently dominate the photovoltaics market. In a recent paper two of the above authors investigated the optical properties of another silicon polytype, the high-pressure phase Si-XII.[5] In this work it was found that the optical absorption coefficient showed a greater overlap with the incident solar spectra than that of three other forms of silicon used for comparison, namely the cubic, amorphous, and polycrystalline forms. This characteristic could result in the material finding use in photovoltaic applications. As another small band gap silicon semiconductor, the bct phase is also expected to have an optical spectrum conducive to its use in photovoltaic applications. Similar expectations are reasonable for bct germanium.

In this paper we first examine the quasiparticle excitation spectra of the bct phases of Si and Ge using the GWA.[3,4] We then solve the Bethe-Salpeter equation for the optical spectra which incorporates the mutual attraction of quasielectrons and quasiholes.[6] Taking into account this mutual interaction can be crucial when comparing to experimental measurements.[6–10] We then examine the optical spectra of these materials and compare the bct phases to their cubic counterparts.

II. METHOD

We have performed *ab initio* pseudopotential calculations within the framework of density-functional theory (DFT) in the LDA to the exchange-correlation functional. The interaction of the valence electrons with the ion cores is represented by a norm-conserving pseudopotential.[11] These calculations are used to evaluate total energies, for structural optimization and as inputs to the subsequent quasiparticle and many-body calculations. The electronic wave functions are expanded in a plane-wave basis[12,13] with a kinetic-energy cutoff of 30 Ry.

Quasiparticle spectra are calculated in the "one-shot" *GW* approximation to the electron self-energy following Hybertsen and Louie.[4] In this approach, the self-energy is approximated by the product of the single-particle Green's function

and the screened interaction.[3] The Green's function is approximated using states and energies resulting from the LDA calculations and the frequency-dependent dielectric matrix needed to compute the screened interaction is obtained by extending the static dielectric matrix to finite frequencies using a generalized plasmon-pole model.[4] This approach has been seen to dramatically improve the agreement with experiment with regards to the band gap of materials than results from simply interpreting the DFT eigenvalues as the quasiparticle energies.

In order to calculate the optical spectra of materials accurately from first principles, the effects of the electron-hole interaction must be included. This necessitates going beyond the quasiparticle calculations discussed above to examine excitations that are characterized by linear combinations of free quasielectron and quasihole pair configurations. These excitations, denoted by $|S\rangle$, are given by

$$|S\rangle = \sum_{\mathbf{k}} \sum_{v}^{hole} \sum_{c}^{elec} A^{S}_{vc\mathbf{k}} \hat{a}^{\dagger}_{v\mathbf{k}} \hat{b}^{\dagger}_{c,\mathbf{k}+\mathbf{Q}} |0\rangle, \quad (1)$$

where $\hat{a}^{\dagger}_{v\mathbf{k}}$ creates a quasihole in state $\mathbf{k}$ and $\hat{b}^{\dagger}_{c,\mathbf{k}+\mathbf{Q}}$ creates a quasielectron in state $\mathbf{k}+\mathbf{Q}$ following the absorption of a photon with wave vector $\mathbf{Q}$. These states and their corresponding energies Ω_S can be calculated by solving the equation of motion for the two-body Green's function using the Bethe-Salpeter equation:[14]

$$(E^{QP}_{c,\mathbf{k}+\mathbf{Q}} - E^{QP}_{v\mathbf{k}}) A^{S}_{vc\mathbf{k}} + \sum_{\mathbf{k}'} \sum_{v'}^{hole} \sum_{c'}^{elec} \langle vc\mathbf{k}|K^{eh}|v'c'\mathbf{k}'\rangle A^{S}_{v'c'\mathbf{k}'} = \Omega_S A^{S}_{vc\mathbf{k}}. \quad (2)$$

The solution of this equation in the limit of $Q \rightarrow 0$ is performed within the framework described by Rohlfing and Louie.[6] Once this equation is solved for the correlated electron-hole excitations $|S\rangle$ and their energies, it is possible to evaluate the optical spectrum.

III. RESULTS AND DISCUSSION

The structures of bct Si and Ge are described in the original work of Fujimoto *et al.*[1] We have relaxed the structures from their original parameters and find that their original structural description is consistent with ours. The calculated gaps in the bct phase are shown in Table I where they are compared with the results of Fujimoto *et al.*[1] The calculated values of the gaps within the local-density approximation are in good agreement. We note, however, that our indirect LDA gap is somewhat larger that that calculated in Ref. 1 for bct Ge. As in Ref. 1, we find the direct gap to be at the Z point for both materials. The indirect gap is between the top of the valence band at Z, for both materials, and the bottom of the conduction band which is along a line connecting Γ to Z in the case of Si and at the P point in the case of Ge.[1]

Despite the good agreement between the calculated values of the gaps within the LDA, the values of the gaps calculated within the *GW* approximation are noticeably different. The values calculated in the present work are larger by an average of 0.38 eV. This difference may be attributed to the different implementations of the *GW* approximation used in calculating the effect of the electron self-energy. As discussed earlier, in this work we utilize a plane-wave implementation of the GWA in which the static dielectric matrix is extended to finite frequencies with the use of a generalized plasmon-pole model.[4] We calculate the static dielectric matrix $\epsilon^{-1}_{G,G'}(\mathbf{q},\omega=0)$ up to a kinetic-energy cutoff of 24 Ry and the self-energy Σ by summing over 59 q points in the irreducible Brillouin zone and 700 bands (8 occupied and 692 unoccupied). In contrast, the calculations done in Ref. 1 are implemented in an all-electron, augmented-wave implementation of GWA using eigenfunctions generated by the full-potential linear muffin-tin orbital (FP-LMTO) method.[1,15] In addition to this difference, the calculations of Ref. 1 also involve the computation of the full-frequency dependence of the screened Coulomb interaction W and do not make use of the plasmon-pole approximation.[15] It is found that in the method of the present work, the calculated band gap of cubic silicon is 1.27 eV whereas that found in Ref. 1 is 1.03 eV (experimental measurement is 1.17 eV). This difference in the results of the two methods is also seen in other calculations in the literature, giving an indication of the precision of this approach. The original calculations of Hybertsen and Louie[4] find a indirect gap of 1.29 eV in the case of cubic silicon whereas calculations done by Faleev *et al.* using the FP-LMTO method find a one-shot *GW* energy gap of 0.84 eV.[16] Thus the fact that we find the bct quasiparticle gap to be somewhat larger in our pseudopotential plane-wave approach than that found in Ref. 1 using an all-electron implementation is consistent with previous results.

TABLE I. The minimum indirect gap E_i and direct gap E_d of bct Si and bct Ge calculated within the LDA and within the GWA. The results from the present work are compared with those found by Fujimoto *et al.* (Ref. 1).

	E_i (eV)		E_d (eV)	
	Ref. 1	Present work	Ref. 1	Present work
bct Si (LDA)	0.10	0.15	0.25	0.32
bct Si (GWA)	0.47	0.86	0.74	1.07
bct Ge (LDA)	−0.39	−0.23	0.11	0.15
bct Ge (GWA)	−0.12	0.38	0.51	0.79

The difference in the magnitude of the quasiparticle corrections for the bct phases from the current work and that of Ref. 1 gives rise to a qualitative difference in the nature of the gap in the case of germanium. In Ref. 1 it was found that bct Ge is semimetallic with an indirect overlap of 0.12 eV. Our calculations suggest that the indirect overlap present in the LDA is increased to an indirect gap of 0.38 eV, thereby predicting that bct Ge should be a small band gap semiconductor. It should be noted that this conclusion does not rest on the fact that the calculations of Ref. 1 find a somewhat larger overlap in the LDA as our calculated quasiparticle corrections are larger than that of Ref. 1 by more than the difference between our LDA indirect gaps. However, it is important to note that in the quasiparticle calculations for

germanium, the occupancies of the states are as they would be in the semiconducting case. This avoids the complexity of representing the intraband transitions in the small region of overlap where the Fermi level crosses the band in the LDA as it would in a true metal.

Once the quasiparticle spectrum has been obtained, we are in a position to solve the Bethe-Salpeter equation (BSE) shown in Eq. (2). We have included all 8 valence bands ($v=1-8$) and the lowest 12 conduction bands ($c=9-20$) in our solution. The calculation of the electron-hole interaction matrix elements is a computationally intensive step and so they are calculated on a coarse grid of 512 **k** points before an interpolation procedure is used to obtain them on a finer grid of 1000 **k** points.[6] We then solve the BSE yielding the coupled excitations $|S\rangle$ and the associated energies Ω_S.

Once these excitations have been solved for using the BSE, the optical spectrum can be evaluated. The imaginary part of the dielectric function, $\epsilon_2(\omega)$, is calculated using

$$\epsilon_2(\omega) = \frac{16\pi^2 e^2}{\omega^2} \sum_S |\vec{\lambda} \cdot \langle 0|\vec{v}|S\rangle|^2 \delta(\omega - \Omega_S). \quad (3)$$

In this expression $\vec{\lambda}$ is the polarization of the incident light and $\vec{v}$ is the single-particle velocity operator. In the absence of electron-hole interactions, Eq. (3) reduces to the following expression involving photon-induced direct transitions between the independent electron and hole states

$$\epsilon_2^{(0)}(\omega) = \frac{16\pi^2 e^2}{\omega^2} \sum_{v,c} |\vec{\lambda} \cdot \langle v|\vec{v}|c\rangle|^2 \delta[\omega - (E_c - E_v)], \quad (4)$$

where the superscript is used to distinguish the fact that electron-hole interactions are not included.

In Fig. 1 we plot $\epsilon_2(\omega)$ for silicon and germanium in the bct structure using the method described earlier. For both materials it is clear that the electron-hole interaction shifts the spectra to lower energies. This behavior is seen in other semiconductors and occurs not because of a shift to lower energies due to the attractive electron-hole interaction but rather due to a constructive superposition at lower energies of the noninteracting matrix elements that make up the coupled excitations $|S\rangle$.[6]

In comparing the absorption spectra between these two materials it is interesting that while both materials have direct gaps near 1 eV, only the germanium phase has any substantial weight in this energy region. The cause of this can be understood by examination of Fig. 2. In Fig. 2 we have plotted the joint density of states (divided by ω^2 to make it comparable to the absorption spectra in Fig. 1) as well as the average squared matrix element, $|\vec{\lambda} \cdot \langle v|\vec{v}|c\rangle|^2$, as a function of energy. While the joint density of states for the two materials are extremely similar, the average squared matrix element for the silicon phase is very small up until after 2.5 eV, which explains why the absorption curve in Fig. 1 does not become substantial until around this energy.

In order to obtain a measure of the possible utility these phases have for photovoltaic applications, we compare the absorption spectra with their cubic counterparts. The cubic phases of both silicon and germanium find widespread use in photovoltaic applications. Silicon-based solar cells dominate

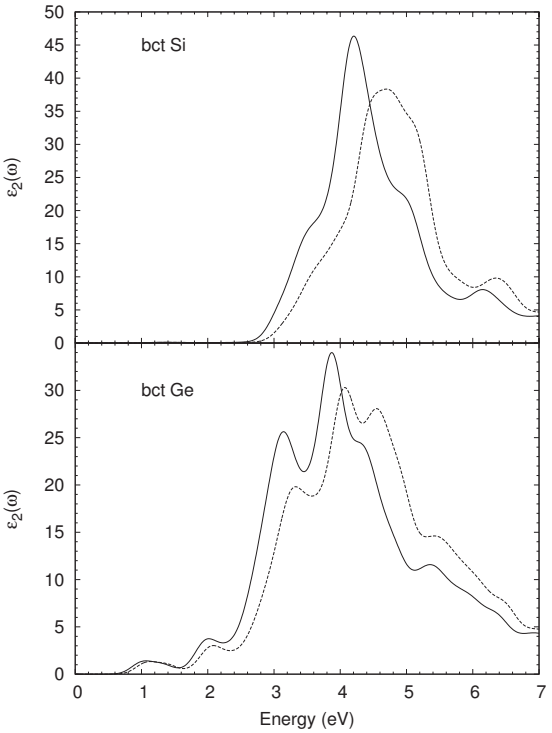

FIG. 1. Calculated $\epsilon_2(\omega)$ of the bct phase of silicon (upper panel) and germanium (lower panel). The solid line is including electron-hole interactions [Eq. (3)] while the dotted line is the noninteracting calculation [Eq. (4)].

the photovoltaics market while germanium is a component in highly efficient multijunction solar cells.[17] While the efficiency of a solar cell certainly depends on other characteristics, our analysis will focus only on the overlap of the absorption coefficient with the incident solar spectrum. In Fig. 3 we plot $\epsilon_2(\omega)$ for silicon in the bct and cubic structures calculated using the method described in this work. The experimental dielectric function for cubic silicon is taken from Ref. 18 and shows the reliability of the method in calculating optical spectra from first principles. The calculations for cubic silicon also show good agreement with others in the literature.[8,9] The calculated $\epsilon_2(\omega)$ for bct silicon shows more weight than cubic silicon at the lowest energies for which the dielectric function is nonzero. However, above ~3.3 eV the value for the cubic phase has a greater magnitude. In terms of the relevance of these curves to photovoltaic absorption in materials, the important energy range is that for which the incident solar flux is appreciable.

In Fig. 4 we show the calculated absorption coefficients of silicon in the bct and cubic phase. Shown also is the air mass (AM) 1.5 solar spectral irradiance.[19] It can be seen that the absorption coefficient of bct silicon is larger for energies where the incident photon flux is greater. The more complete the overlap between the absorption coefficient and the incident solar spectrum the less material that is needed to capture a given quantity of light. It is also important to note that in the calculations only direct transitions are taken into account. With the inclusion of phonon-assisted, i.e., indirect, transitions we would expect the absorption coefficient of silicon in the bct phase to have a finite values at lower energies than

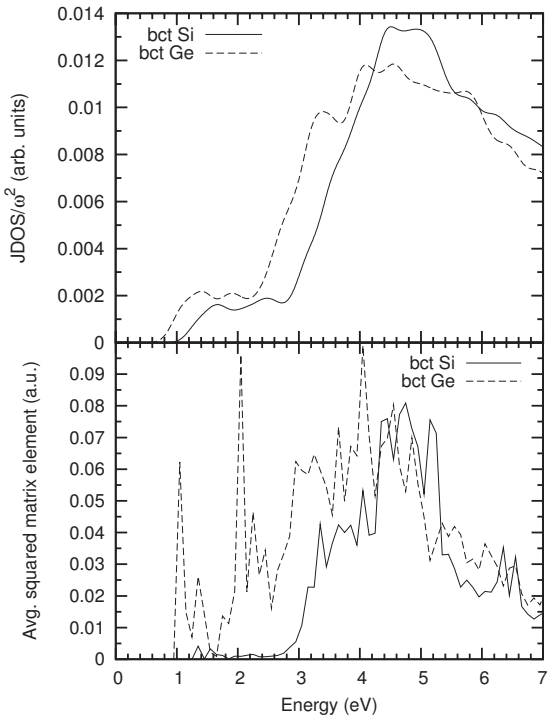

FIG. 2. Upper panel: calculated joint density of states (JDOS), divided by ω^2, for silicon and germanium in the bct phase. Lower panel: average squared matrix element $|\vec{\lambda}\cdot\langle v|\vec{v}|c\rangle|^2$ for the two calculations. The size of the energy bins in the lower panel is 0.1 eV.

for the case of cubic silicon arising from the smaller indirect band gap found in the bct phase. While there are other considerations that must be taken into account when building a solar device, the strong overlap between the absorption coefficient of bct silicon and the solar spectrum owing to the smaller band gap of this form of silicon shows promise for use in photovoltaic devices.

We now turn to the case of germanium in the bct phase. In Fig. 5 we show the calculated $\epsilon_2(\omega)$ for germanium in the bct structure compared with experimental data on its cubic phase from Ref. 20. Compared to its cubic counterpart, bct Ge

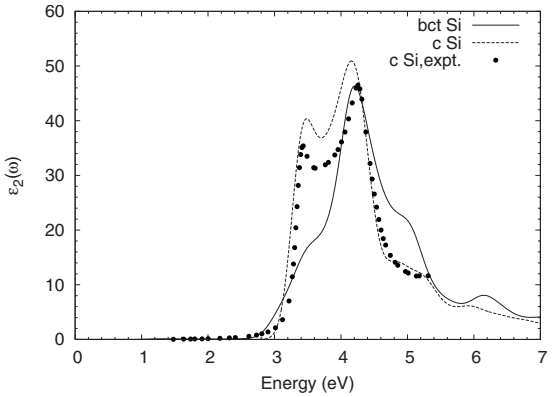

FIG. 3. Calculated $\epsilon_2(\omega)$ of silicon in the bct and cubic phases. The calculated curve for cubic silicon (cSi) is compared to the experimental data from Ref. 18 and indicates the reliability of the present method for calculating optical spectra. The calculated curves include an artificial broadening of 0.15 eV.

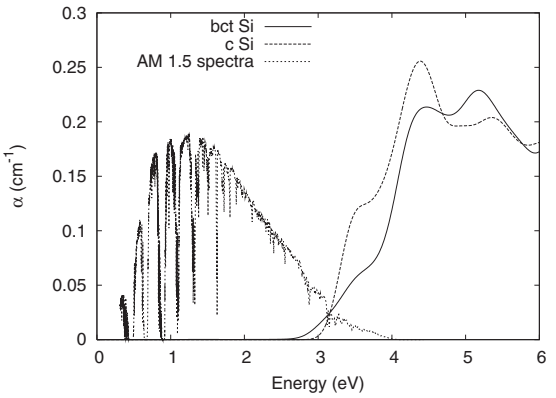

FIG. 4. Calculated optical absorption coefficient α of silicon in the bct and cubic structures. Shown also in arbitrary units is the solar spectral irradiance for AM 1.5.

appears to have substantially less weight at lower energies at which the incident solar flux is large. Thus even though germanium's bct phase compares favorably to the bct phase of silicon as seen in Fig. 1, the fact that the cubic phase of Ge has a much smaller direct gap of 0.89 eV compared to the direct gap of 3.4 eV in cubic silicon[21,22] results in the bct Ge phase comparing unfavorably in terms of overlap with the solar spectrum whereas the bct Si phase compares favorably in relation to their respective cubic counterparts.

In conclusion we have calculated the quasiparticle excitation and optical absorption spectra of the recently predicted bct phase of silicon and germanium. The quasiparticle spectra are calculated using a plane-wave implementation of the *GW* approximation which predict that both Si and Ge in the bct structure are semiconductors with indirect gaps of 0.86 and 0.38 eV, respectively. The optical absorption spectrum is obtained by solving the Bethe-Salpeter equation to take into account the effect of the electron-hole interactions. The obtained optical coefficients of silicon in the bct structure show a better overlap with the incident solar spectrum than do those for the cubic structure. In addition to providing optical characterization of this predicted silicon and germanium polytype, the calculations suggest that this phase of silicon may find possible applications within the realm of photovoltaics.

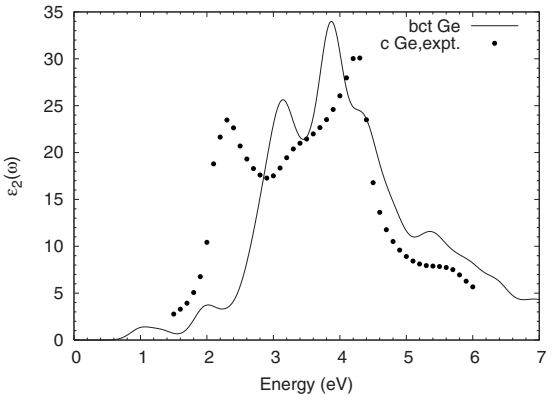

FIG. 5. Calculated $\epsilon_2(\omega)$ of germanium in the bct and compared to experimental data on cubic germanium taken from Ref. 20. The calculated curves include an artificial broadening of 0.15 eV.

ACKNOWLEDGMENTS

The authors would like to thank Susumu Saito and Georgy Samsonidze for helpful discussions. This work was supported by National Science Foundation Grant No. DMR07-05941 and by the Director, Office of Science, Office of Basic Energy Sciences, Division of Materials Sciences and Engineering Division, U.S. Department of Energy under Contract No. DE-AC02-05CH11231. Computational resources have been provided by NERSC and NPACI.

*bmalone@civet.berkeley.edu

[1] Y. Fujimoto, T. Koretsune, S. Saito, Y. Miyake, and A. Oshiyama, New J. Phys. **10**, 083001 (2008).
[2] Y. Omata, Y. Yamagami, K. Tadano, T. Miyake, and S. Saito, Physica E **29**, 454 (2005).
[3] L. Hedin and S. Lundqvist, in *Solid State Physics*, edited by F. Seitz, D. Turnbull, and H. Ehrenreich (Academic Press, New York, 1969), Vol. 23.
[4] M. S. Hybertsen and S. G. Louie, Phys. Rev. B **34**, 5390 (1986).
[5] B. D. Malone, J. D. Sau, and M. L. Cohen, Phys. Rev. B **78**, 161202(R) (2008).
[6] M. Rohlfing and S. G. Louie, Phys. Rev. B **62**, 4927 (2000).
[7] G. Onida, L. Reining, R. W. Godby, R. DelSole, and W. Andreoni, Phys. Rev. Lett. **75**, 818 (1995).
[8] S. Albrecht, L. Reining, R. DelSole, and G. Onida, Phys. Rev. Lett. **80**, 4510 (1998).
[9] L. X. Benedict, E. L. Shirley, and R. B. Bohn, Phys. Rev. Lett. **80**, 4514 (1998).
[10] J. W. van der Horst, P. A. Bobbert, M. A. J. Michels, G. Brocks, and P. J. Kelly, Phys. Rev. Lett. **83**, 4413 (1999).
[11] J. P. Perdew and A. Zunger, Phys. Rev. B **23**, 5048 (1981).
[12] J. Ihm, A. Zunger, and M. L. Cohen, J. Phys. C **12**, 4409 (1979).
[13] M. L. Cohen, Phys. Scr. **T1**, 5 (1982).
[14] G. Strinati, Phys. Rev. B **29**, 5718 (1984).
[15] T. Kotani and M. van Schilfgaarde, Solid State Commun. **121**, 461 (2002).
[16] S. V. Faleev, M. van Schilfgaarde, and T. Kotani, Phys. Rev. Lett. **93**, 126406 (2004).
[17] F. Dimroth and S. Kurtz, MRS Bull. **32**, 230 (2007).
[18] G. E. Jellison, Jr., Opt. Mater. (Amsterdam, Neth.) **1**, 41 (1992).
[19] A. S. T. M. Standard, G173, "Standard Tables for Reference Solar Spectral Irradiances: Direct Normal and Hemispherical on 37 Degree Tilted Surface." ASTM International, West Conshohocken, PA, DOI:10.1520/G0173-03E01, www.astm.org
[20] D. E. Aspnes and A. A. Studna, Phys. Rev. B **27**, 985 (1983).
[21] D. E. Aspnes, Phys. Rev. B **12**, 2297 (1975).
[22] D. Straub, L. Ley, and F. J. Himpsel, Phys. Rev. Lett. **54**, 142 (1985).